Analytic proof that the quark model complies with partially conserved axial current theorems

Pedro Bicudo
Departamento de Física, and CFIF, Instituto Superior Técnico, Av. Rovisco Pais, 1049-001 Lisboa, Portugal
(Received 22 October 2001; revised manuscript received 30 January 2002; published 6 March 2003)

The Weinberg theorem, the Adler self-consistency zero, the Goldberger and Treiman relation, and the Gell-Mann, Oakes, and Renner relation are proved analytically in full detail for quark models. These proofs are independent of the particular quark-quark interaction, and they are displayed with Feynman diagrams in a compact notation. I assume the ladder truncation, which is natural in the quark model, and also detail the diagrams that must be included in each relation. Off mass shell and finite size effects are included in the quark-antiquark pion Bethe-Salpeter vertices. The axial and vector Ward identities, for the quark propagator and for the ladder, exactly cancel any model dependence.

DOI: 10.1103/PhysRevC.67.035201 PACS number(s): 24.85.+p, 12.39.Jh

I. INTRODUCTION

The pion was introduced by Yukawa in 1931 to account for the strong nucleon-nucleon attraction which binds the nucleus. Yukawa was inspired by the Coulomb attraction in atomic physics which is due to the photon exchange interaction. The pion was indeed experimentally discovered; it is a pseudoscalar and an isovector. The pion mass $M_{\pi^\pm}=140$ MeV and $M_{\pi^0}=135$ MeV determines the range of the nucleon-nucleon attraction and confirms the prediction of Yukawa. The analogy with photon physics went quite far. The U(1) gauge symmetry is a crucial property of quantum electrodynamics. In hadronic physics there is also a symmetry, chiral symmetry, which is a spontaneously broken global symmetry. In the chiral limit (limit of exact chiral symmetry) the pion would play the role of the massless Goldstone boson. The pion mass is finite but it is indeed much smaller than the mass scale of hadronic physics which is of the order of GeV. The expansion in the pion mass, together with the techniques of current algebra, led to beautifully correct theorems, the PCAC (partially conserved axial current) theorems. Similar to the vector Ward identities in gauge symmetry, the axial Ward identities constitute a powerful tool of chiral symmetry. An important parameter of PCAC is f_π, which relates the pion vertex with the axial vertex. $f_\pi=93$ MeV is measured in the electroweak pion decay, and it is also known as the pion decay constant.

Other hadrons, including hundreds of resonances, were also found subsequently. The large number of hadrons and deep inelastic scattering led to the discovery of quarks and to QCD (quantum chromodynamics), which is the currently accepted theory of strong interactions. QCD has not been solved yet, but it inspired the invention of the quark model [1] in order to describe the bound states of quarks, which fall mainly in the classes of mesons (like the pion) and baryons (like the proton). The quark model also uses confining potentials that are determined in lattice QCD. The success of the quark model relies on its ability to reproduce the whole spectrum of hadronic resonances, with microscopic interacting quarks. Moreover, the quark model is competent to explain microscopically the strong hadron-hadron elastic interactions [2]. For recent coupled channel studies see Refs. [3–5].

However, the quark model suffered from the onset to accommodate the low pion mass. The mass scale of hadronic physics is of the order of GeV. The quark model needed a large number of parameters in order to fit the low pion mass and to address pion creation and annihilation in hadronic decays. It is clear that a light pion is natural in chiral physics, while it is odd in constituent models. With the aim to cure the important problems of pion mass [6,7], pion coupling [8], and vacuum condensate [8], chiral symmetry breaking was introduced in the quark model. This paper continues the program of implementing chiral symmetry in the quark model, showing that the quark model also complies with some of the most famous PCAC theorems. In particular I address the relation of Gell-Mann, Oakes, and Renner [9], the Goldberger-Treiman relation [10], the Adler self-consistency zero [11], and the Weinberg theorem [12].

I do not aim to derive new theorems here for pion physics. Since the pioneering work of Yukawa, pion properties have already been understood through the techniques of current algebra, the σ model, the Nambu–Jona-Lasinio model, and chiral Lagrangians. The goal of this paper is to achieve the same perfect understanding of chiral symmetry breaking in the quark model. This understanding is not trivial in the quark model because the pion is an extended [13] and composite meson, composed of a quark-antiquark pair. Recently Bjorken asked: "How are the many disparate methods of describing hadrons which are now in use related to each other and to the first principles of QCD?" Here the missing link between the quark model and the low energy unique field theory of pions is investigated. This work clarifies what classes of diagrams are necessary to recover the pion theorems in the quark model, and explicitly shows the role of the axial Ward identity in the quark model. This is potentially useful for the numerous hadronic processes that the quark model addresses.

Moreover, it is important to stress that the quark model provides an explicit prescription to address virtual pions with off mass shell momenta. The quark model is suited to describe the virtual exchange of a meson with momentum equal to the sum of the quark and antiquark momenta, and different from the momentum of the mass shell. The relevant experimental processes that I study here are the neutron decay and π-π scattering. In neutron decay a virtual pion is

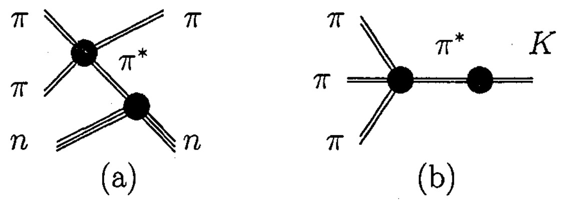

FIG. 1. In (a) a π on mass shell is scattered by a virtual π^* provided by a nucleon. In (b) a virtual pion, which results from a weak flavor change in the incoming K, decays into three pions. Both (a) and (b) contribute to hadronic reactions which are measured in the laboratory.

produced by the nucleon. Moreover, the experiments use at least one virtual pion in π-π scattering because two beams of pions have not yet been scattered in the laboratory. One should acknowledge that it is possible to extract mass shell π-π scattering parameters from pion-nucleon scattering and form kaon to pion-pion decay [14], and that an improvement in data is expected in the new DIRAC [15] experiment at CERN, which will soon be able to measure directly π-π scattering both on the mass shell and at the threshold. Nevertheless there is also interesting data for π-π scattering off the mass shell. For instance, the π-π phase shifts are experimentally estimated with the help of $\pi\ N \to \pi\ \pi\ N$ scattering [16]. In a possible contribution to $\pi\ N \to \pi\ \pi\ N$ at threshold, the nucleon provides a virtual pion π^* with offshellness $P^2 - M_\pi^2 = -3.32 M_\pi^2$ [see Fig. 1(a)]. Another experiment is $K^+ \to \pi^+\ \pi^+\ \pi^-$ where the kaon provides a virtual pion with offshellness $P^2 - M_\pi^2 = +10.75 M_\pi^2$ [see Fig. 1(b)].

The quark model is usually understood with simple quantum mechanics. Baryons are bound states of three quarks, mesons are quark-antiquark bound states, and both are studied with the Schrödinger equation. The hadronic reactions are also studied with coupled-channel equations, and the couplings are computed with the resonating group method. In this paper I choose to display the equations with the compact notation of Feynman diagrams, following the simplifying principles of Llewellyn-Smith in his proof of the Bethe-Salpeter normalization condition [17]. This decreases the number of terms involved in the equations because the Feynman propagator includes both the quark and the antiquark poles,

$$\frac{i}{\not{k} - m + i\epsilon} = \frac{i\Sigma_s u_s u_s^\dagger \beta}{k_0 - E + i\epsilon} - \frac{i\Sigma_s v_s v_s^\dagger \beta}{-k_0 - E + i\epsilon}, \tag{1}$$

where $u_s(\mathbf{k})$ and $v_s(\mathbf{k})$ are the quark and the antiquark Dirac spinors. The translation from the covariant Feynman notation to the nonrelativistic notation *is direct and exact*, and is based on Eq. (1). Incidently the formalism of Feynman diagrams applies straightforwardly to relativistic models such as the Nambu and Jona-Lasinio model [18,19] and other models with Euclidean space integrations [4,20–22] and also to covariant models in Minkowsky space [23].

The essential simplicity of the quark model resides in using *only two-body and finite* quark-antiquark interactions. This is equivalent to using only planar interactions in the possible series of Feynman diagrams, which are also obtained in the large N_c (number of colors) limit of QCD [19]. In particular the intermediate meson exchange is described by the ladder series

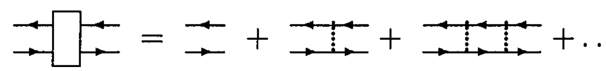

(2)

where the dotted line corresponds to the chiral invariant quark-quark interaction of vertex V and of local kernel $\mathcal{K}$. As usual in the quark model, the vertex V is color dependent and includes a Gell-Mann matrix $\lambda^a/2$. The arrowed line corresponds to the Feynman quark propagator. In this paper the direct coupling of three or four mesons is studied. I use the technique of dressing the corresponding Feynman loop with all possible planar insertions of the quark-antiquark interaction, and to resum the obtained series in terms of the quark-antiquark ladder. Again, the ladder is well defined for any total momentum, and this includes off-mass-shell momenta.

I also assume that chiral symmetry is spontaneously broken in the quark model. This is the only assumption in this paper that goes beyond the minimal quark model. However, the phenomenological success of PCAC shows that it is crucial to include chiral symmetry in the quark model. Therefore, the vertex V is assumed to anticommute with γ_5. Frequently a vector vertex inspired in the gluon coupling is used for V, but other Dirac structures for the vertex V can also be also used [24]. Moreover, the bare quark propagator

$$S_0(k) = \frac{i}{\not{k} + m + i\epsilon} \tag{3}$$

must be replaced, in the computed Feynman loops, by the dressed quark propagator

$$S(k) = \frac{i}{A(k^2)\not{k} + B(k^2) + i\epsilon}, \tag{4}$$

where the functions A and B are nontrivial solutions of the mass gap equation and include the scale of the interaction which is comparable to $\Lambda_{\rm QCD}$. The current quark mass m is much smaller than the scale $\Lambda_{\rm QCD}$, and therefore it only affects pertubatively A and B. In what concerns bound states, the degeneracy of chiral partners is broken, in particular the π is a Goldstone boson in the chiral limit. These basic properties of the quark model with chiral symmetry have been understood for some time through covariant [25,26] quark models with the Schwinger-Dyson equation and through equal-time quark models [6,11,8,27] with the mass gap equation, and therefore they are used as a starting point in this paper.

With the concern of deriving a general proof that the quark model complies with the PCAC relations, I follow in this paper the logical path of using the simplest PCAC relations as the necessary intermediate steps to arrive at the rather technical proof of the Weinberg theorem for π-π scattering. Sections II and III define the formalism of this paper. This formalism is standard; nevertheless it is convenient to define it clearly. Section II reviews mesons as quark-antiquark bound states in the ladder framework. Section III reviews the axial Ward identity which is crucial for the low-energy pion theorems. Sections IV and V apply the techniques defined in Secs. II and III to standard PCAC relations, which have been extensively studied in the literature. This checks the methods used in this paper. Section IV recovers the relation of Gell-Mann, Oakes, and Renner. Section V recovers the Goldberger-Treiman relation. Once the formalism is defined and checked, Secs. VI and VII explicitly study the more technical PCAC relations. Section VI proves that the quark models possess the Adler self-consistency zeros. Section VII proves that the quark models comply with the Weinberg theorem. The conclusion is presented in Sec. VIII.

II. QUARKS, MESONS, AND THE LADDER

The ladder series is a geometrical series which includes bound states. A meson is a quark-antiquark bound state that corresponds to a pole in the series. Outside the pole the ladder does not describe asymptotic states; nevertheless ladder exchange appears as a subdiagram contributing to the interaction of asymptotic states. Then the ladder includes both the off-mass-shell exchange of mesons and the contact interaction term.

I follow the usual convention of factorizing the pole and the Bethe-Salpeter vertices. In the close neighborhood of a bound state b, a pole M_b^2 occurs in the external momentum P^2, and the ladder obeys the spectral decomposition

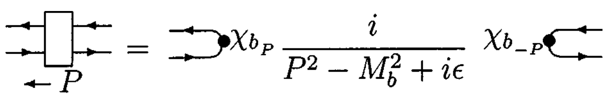

(5)

where

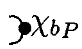

is the Bethe-Salpeter vertex, or truncated amplitude, of a meson, and the arrowed

line represents a dressed quark propagator $\mathcal{S}$. The nonamputated amplitude is simply obtained with the product $\mathcal{S}\chi_{b_P}\mathcal{S}$. Equation (5) and the rest of the paper follows the convention where the momentum P^μ of the vertex flows inside the quark loop, summing to the outgoing quark line. $\chi_{b_{-P}}$ has the opposite total momentum, in particular $-P^0$ is negative. $\chi_{b_{-P}}$ can also be obtained from χ_{b_P} with the charge conjugation transformation. χ_{b_P} is a function of the relative momentum k of the bound pair of a quark and an antiquark.

In what concerns the total four-momentum P^μ, the bound state vertex is straightforwardly defined in the mass shell, which corresponds to the exact momentum of the pole $P^2 = M_b^2$. Nevertheless with Eq. (5) it is possible to extend the definition of χ_{b_P} to a small neighborhood of the pole, up to first order in the off-mass-shell quantity $P^2 - M_b^2$. In diagrammatic language, *the ladder includes both the exchange of mesons and the contact interaction*. The off-mass-shell vertex also includes the principal part of the ladder series. The principal part contains the contact interaction and also contains the infinite tower of excited states, which are a solution of the bound state equation when the potential is confining. Extending the Bethe-Salpeter vertex off the mass shell constitutes an economical method to include all these effects. The off-mass-shell vertex is well defined at least in a small neighborhood of the pole.

To compute the Bethe-Salpeter vertex, it is convenient to rewrite the ladder in a self-consistent equation,

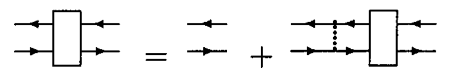

(6)

Replacing Eq. (5) in Eq. (6), and folding it from the left with χ_P, the off-mass-shell Bethe-Salpeter equation is obtained,

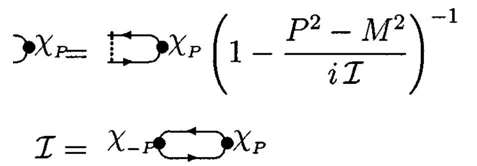

$$= \int tr\{\chi_P(k)\mathcal{S}(k+P/2)\chi_{-P}(k) \times \mathcal{S}(k-P/2)\} , \tag{7}$$

where $\mathcal{I}$ is both displayed as a Feynman loop and as an integral. For compactness, the convention of representing integrals of propagators and vertices with Feynman diagrams will mainly be used in the rest of the paper. The loop $\mathcal{I}$ is finite and proportional to the square of the scale of the interaction. Nevertheless $\mathcal{I}$ will factorize from the results of this paper, which are model independent. At the mass-shell momentum, Eq. (7) simplifies to the standard Bethe-Salpeter equation,

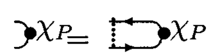

(8)

To check that the off mass shell Eq. (7) Bethe-Salpeter equation is correct, I derive from it the normalization condition [17] for the Bethe-Salpeter vertices. Folding from the right with χ_{-P}, Eq. (7) becomes

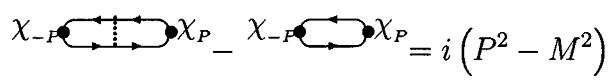

(9)

and the correct normalizing condition is obtained when Eq. (9) is derived by $\partial/\partial P^\mu$. The derivative of the left-hand side is

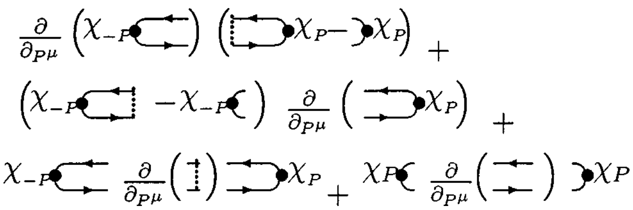

(10)

and this provides a general normalizing condition for the vertex. Frequently mass shell vertices and local kernels are used. Then the Bethe-Salpeter equation (8) can be used to precisely cancel the terms with the derivative of the vertices χ_P and χ_{-P}, and the derivative of the kernel also vanishes because the kernel (the quark-quark interaction) is local. With these cancellations, the derivative of Eq. (9) is simply

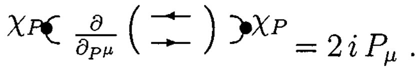

(11)

This is the standard normalizing condition for mass shell Bethe-Salpeter vertices with a local kernel.

The off-mass-shell equation (7) is particularly simple in the case where the bound state is a low-energy pion. In this case the expansion in the external P^μ and in M_π can be used, because M_π and P^μ are much smaller that the characteristic scale of meson physics, say $2\Lambda_{\rm QCD}$. The off-mass-shell correction only starts contributing to the Bethe-Salpeter equation (7) at the second order of P^2 and M^2. Therefore, up to the first order in P^μ and in M_π, the vertex χ_P is *formally the same function* of P^μ, both for mass-shell and for off-mass-shell pions. For instance, the momentum expansion up to first order in P^μ of the pion Bethe-Salpeter vertex

$$\chi_P(k)=\chi^0(k)+P^\mu\chi^1_\mu(k)+o(P^\mu P^\nu),$$
$$\chi^1_\mu(k)=\{F(k)\gamma_\mu+G(k)k_\mu \not{k}+H(k)[\gamma_\mu,\not{k}]\}\gamma_5 \quad (12)$$

is also correct, and formally the same, for any small off-mass-shell momentum P^μ. In particular the expansion in P^μ of the Bethe-Salpeter equation (8) yields for $\chi^0(k)$ and for the components of $\chi^1_\mu(k)$ four equations totally independent of P^μ. $\chi^0(k)$ will be exactly derived in Eq. (23). Importantly, the four components of χ_π will only contribute to the PCAC theorems of this paper through the pion decay constant f_π, which is defined by the trace

$$\mathrm{tr}\{(S\chi S)_P\gamma^\mu\gamma^5\}=\sqrt{2}f_\pi P^\mu, \quad (13)$$

where $\sqrt{2}$ is a flavor factor. In Eq. (13) and in the rest of the paper the traces are assumed to include the momentum integral and the sum in Dirac and color indices. The important result of this low-energy pion discussion is that Eq. (13) is also correct outside the mass shell for $P^2\neq M^2$ when a virtual intermediate pion is used, providing the momentum P^μ is small.

I now derive a second important relation, which states how to include (or remove) a ladder in the vertex χ_P. Folding Eq. (5) from the right with the vertex χ_P, and dividing by the $\mathcal{I}$ loop,

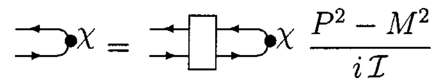

(14)

III. USING THE AXIAL WARD IDENTITY

When chiral symmetry breaking occurs, the mass gap equation has a nontrivial solution. The Schwinger-Dyson equation for the full propagator is

$$S(k)^{-1}=S_0^{-1}(k)+i\int\frac{d^4q}{(2\pi)^4}\mathcal{K}(q)VS(k+q)V. \quad (15)$$

Equation (15) is also known as the mass gap equation because the initially almost massless gap between the quark and antiquark dispersion relations is increased when the constituent mass $M=\sqrt{B^2/A^2}$ is generated. Because the vertex V includes the Gell-Mann matrices, the tadpole does not contribute to Eq. (15). Multiplying Eq. (15) right or left with γ_5 and summing leads to

$$S(k_1)^{-1}\gamma_5+\gamma_5S(k_2)^{-1}$$
$$=S_0(k_1)^{-1}\gamma_5+\gamma_5S_0(k_2)^{-1}-i\int\mathcal{K}(q)V[S(k_1+q)$$
$$\times\gamma_5+\gamma_5S(k_2+q)]V, \quad (16)$$

which is the Bethe-Salpeter equation for the vertex

$$\Gamma_A(k_1,k_2)=\gamma_A(k_1,k_2)-i\int\frac{d^4q}{(2\pi)^4}\mathcal{K}(q)VS(k_1+q)\Gamma_A(k_1$$
$$+q,k_2+q)S(k_2+q)V, \quad (17)$$

and this shows [26,7,24,28,27] that the ladder approximation for the bound state is consistent with the quark self-energy equation in the rainbow approximation. Both approximations are equivalent to the planar diagram expansion, which is characteristic of the quark model.

In the Bethe-Salpeter equation (17), the bare and dressed vertices are defined by the same axial Ward identity

$$\Gamma_A(k_1,k_2)=S^{-1}(k_1)\gamma_5+\gamma_5S^{-1}(k_2),$$
$$\gamma_A(k_1,k_2)=S_0^{-1}(k_1)\gamma_5+\gamma_5S_0^{-1}(k_2). \quad (18)$$

At this point it is important to clarify that in the chiral limit of $m=0$, the bare vertex γ_A is essentially the momentum contracted with the bare axial vertex $\gamma^\mu\gamma_5$, and in the limit of vanishing momentum P_μ, the vertex γ_A is essentially the current quark mass times the bare pseudoscalar vertex γ_5. In general, γ_A is a combination of the axial vertex and the pseudoscalar vertex. In what concerns the dressed vertex Γ_A, it will be used up to second order in the total momentum, and in general the Dirac structure of Γ_A has four components, similar in structure to the four components of the pion Bethe-Salpeter vertex (12). Therefore this vertex cannot be reduced in the quark model framework, neither to a pure pseudoscalar term nor to a pure axial vector term. Nevertheless in the rest of this paper, for simplicity and because they are defined with the axial Ward identity (18), γ_A will be called the bare axial vertex and Γ_A will be called the dressed axial vertex, although they possess a more general Dirac structure.

The bare axial vertex γ_A is computed from the bare quark propagator (3):

$$\gamma_{A_P}=\frac{(\not{P}-2m)}{i}\gamma_5, \quad P=k_1-k_2. \tag{19}$$

γ_A is the particular part of the Bethe-Salpeter equation for the vertex (17), and it vanishes when the current quark mass m is small (chiral limit) and at the same time the total momentum P^μ of the vertex is small. On the other hand, the dressed vertex Γ_A is computed from the dressed quark propagator (4),

$$\Gamma_A(k_1,k_2)=\frac{A(k_1)\not{k}_1-A(k_2)\not{k}_2-B(k_1)-B(k_2)}{i}\gamma_5. \tag{20}$$

Γ_A is finite, provided spontaneous chiral symmetry breaking occurs in Eq. (15) to generate a dynamical mass in the dressed quark propagator. For instance, when the total momentum $P=k_1-k_2$ of the vertex vanishes, the vertex is simply identical to $2i\ B(k)\gamma_5$, where $B(k)$ is a finite solution of the mass gap equation.

For simplicity the flavor is not yet included. Flavor will only be explicitly included at the end of Sec. VII. The isoscalar axial Ward identity must include the axial anomaly, which is crucial to the U(1) problem. Nevertheless the pion is an isovector, and in the coupling of a pion I do not need to be concerned with the axial anomaly.

I now derive two powerful relations which involve the axial vertices and the ladder. After iterating the Bethe-Salpeter equation (17) for the dressed axial vertex Γ_A, and including the external propagators, a first useful relation is derived,

$S\,\Gamma_A\,S=$ 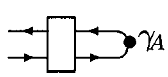 . (21)

To derive some of the PCAC proofs it is crucial to use a second relation which is an extension of Eq. (18),

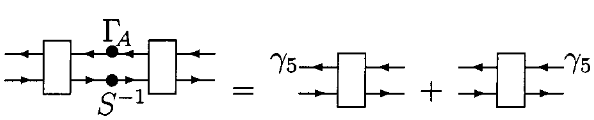

(22)

and this constitutes a Ward identity for the ladder. This identity is derived if I expand [27] the ladders and substitute the vertex in the left-hand side. Then all terms with an intermediate γ_5 include the anticommutator $\{\gamma_5,V\}$ and this cancels because *the interaction is chiral invariant* and *the kernel is local*. Only the right-hand side survives.

IV. THE GELL-MANN, OAKES, AND RENNER RELATION

In the limit of vanishing current quark mass m and vertex momentum P^μ, the Bethe-Salpeter equation (17) for the axial vertex Γ_A becomes homogeneous and is thus identical to a homogeneous Bethe-Salpeter equation (8) for a pion vertex $\chi_{\pi^P}(k)$ with vanishing mass. In this limit the pion is a massless Goldstone boson, and the pion Bethe-Salpeter vertex is proportional to the dressed axial vertex, and to the dynamical quark mass $B(k)$,

$$\chi_0(k)=\frac{B(k)}{n_\pi}\gamma_5=\frac{1}{2in_\pi}\Gamma_{A0}(k,k), \tag{23}$$

where n_π is the norm of the pion vertex, which is defined by Eq. (11). This can also be checked by the relation

$$V\mathcal{S}(k)B(k)\gamma_5\mathcal{S}(k)V=V\frac{B(k)}{A(k)^2k^2-B(k)^2}V\gamma_5, \tag{24}$$

which explicitly verifies that the integrand of the Bethe-Salpeter equation for the pion vertex, in the limit vanishing current quark mass m and vertex momentum P^μ, is identical to the integrand of the Schwinger-Dyson equation for the scalar component B of the dressed quark propagator. It is important to remark that outside this limit Eq. (23) does not hold, but the difference between the pion vertex and the axial vertex only starts to contribute at first order in the expansion in m and P^μ,

$$\chi_P(k)=\frac{1}{2in_\pi}\Gamma_{A_P}(k)+o(P^\mu,m). \tag{25}$$

Substituting the spectral decomposition [25] of the ladder (5), Eq. (21) implies that

$$\begin{aligned}\Gamma_{A_P}&=\chi_P\frac{i}{P^2-M_\pi^2}\mathrm{tr}\{\chi_{-P}(S\gamma_A S)_P\},\\ &\simeq\frac{1}{2in_\pi}\Gamma_A\frac{i}{P^2-M_\pi^2}\mathrm{tr}\{(S\chi S)_{-P}\gamma_{A_P}\},\end{aligned} \tag{26}$$

where only the first nonvanishing terms in the expansion in P^μ and in M_π is retained. In particular the pion vertex in the left-hand side was simplified with Eq. (23). The leading result is

$$\mathrm{tr}\{(S\chi S)_{-P}\gamma_{A_P}\}=2n_\pi(P^2-M_\pi^2). \tag{27}$$

It is also convenient to extend this result to the case where different external momenta are involved in $(S\chi S)$ and in γ_A. A detailed momentum analysis of Eqs. (13), (19), and (27) shows that the norm $n_\pi=if_\pi/\sqrt{2}$ and produces [28] the desired trace:

$$\mathrm{tr}\{(S\chi S)_{P_1}\gamma_{A_{P_2}}\}=-2n_\pi(P_1\cdot P_2+M_\pi^2). \tag{28}$$

Using Eqs. (14), (19), and (28) when the momenta vanish, an important particular result is derived:

$$2m\,\mathrm{tr}\{S\}=f_\pi^2M_\pi^2, \tag{29}$$

where $-\mathrm{tr}\{S\}$ is the quark condensate $\langle\bar{\psi}\psi\rangle$. Equation (29) is the relation of Gell-Mann, Oakes, and Renner [9]. In the

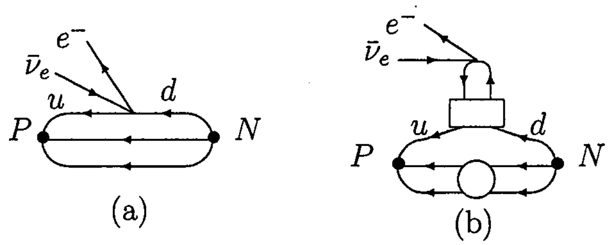

FIG. 2. This figure shows the microscopic description of the weak decay $N \to P + e^- + \overline{\nu_e}$, where a d quark produces a u quark and two leptons with the four Fermi weak coupling. The bare diagram is depicted in (a) and the corresponding fully dressed diagram is depicted in (b). (b) includes a full ladder, which is represented with a full box, and the series of interactions of the diquark which is not coupled to the leptons, which is represented with an empty circle.

chiral limit the quark condensate $\langle \overline{\psi}\psi \rangle$ and the pion decay constant f_π remain constant. The relation of Gell-Mann, Oakes, and Renner shows that the pion mass M_π is proportional to $\sqrt{m}$. This relation can also be extended [29–31] for arbitrarily large current-quark masses, and this provides, for instance, an intuitive understanding of modern lattice simulations.

V. THE GOLDBERGER-TREIMAN RELATION

The Goldberger-Treiman relation provides a convenient exercise to resum the series of planar diagrams, to describe the intermediate virtual meson exchange with the ladder, and to check that the pion vertex can be used outside the mass shell. The weak decay of the neutron, $n \to p + e^- + \overline{\nu_e}$ is computed with Feynman diagrams that include the four Fermi coupling of two quark legs with the electron and the neutrino leg. The bare loop of Fig. 2(a) does not correctly account for the strong interaction. A complete set of insertions of the quark-quark potential must be used. However, three classes of insertions are included from the onset. The vertex V of the quark-quark potential is assumed to be already renormalized and should not be further dressed. For instance, renormalizing diagrams for V have not been used neither in the mass gap equation (15) nor in the ladder series (6). The propagator S is also dressed; it is a solution of the mass gap equation (15). Moreover, the Bethe-Salpeter vertices χ of the proton and neutron are already dressed; they are solutions of the three-body Bethe-Salpeter equation. However, the four Fermi coupling is not dressed from the onset and it remains to be dressed. A detailed inspection shows that the full series of planar diagrams can be resummed in a ladder series that dresses [32–34] the Fermi coupling, and in interactions in the remaining diquark of the nucleon. The ladder series is represented by a box in Fig. 2(b). The interactions in the remaining diquark of the nucleon are represented by an open circle in Fig. 2(b); however, they will not affect the results of this paper.

When the ladder in Fig. 2(b) is replaced by the spectral decomposition of Eq. (5), the dressed Feynman loop (b) factorizes in the product of the coupling of a nucleon to a pion $N \to P + \pi^-$, of the pion propagator, and of the electroweak decay of the pion $\pi^- \to e^- + \nu_e$ [26]. The axial part of the electroweak decay can be measured, and I just have to compute the coupling of $P_1^\mu \gamma_\mu \gamma_5$ to a quark line of the nucleon. This is included in the bare axial vertex γ_A, and it is convenient to compute

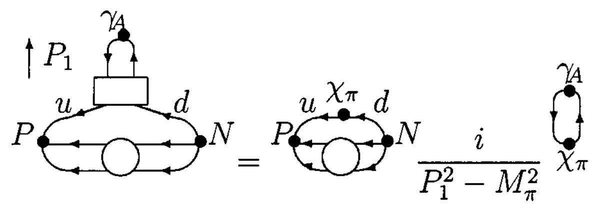

(30)

Summing the contribution of the three quarks internal to the proton and the neutron, the left-hand side of Eq. (30) is identical to $\sqrt{2} M_n g_A / i$. This is defined in nuclear physics from the Dirac equation for the nucleon, which is considered as a Dirac fermion. The vertex γ_A can be rewritten as $(\not{k}_P \gamma_5 + \gamma_5 \not{k}_N - 2m\gamma_5)/i$, where k_P is the momentum of the quark that flows into the proton and k_N is the momentum of the quark that comes from the neutron. Summing the contribution of the three quarks to this amplitude, and interpreting the nucleon as a Dirac particle, the left-hand side of Eq. (30) is identical to the matrix element of $(\not{P}_P \gamma_5 + \gamma_5 \not{P}_N - 6m\gamma_5)/i$. Continuing to interpret the nucleon as a Dirac particle the proton and nucleon slashed momenta can be replaced, respectively, by M_N and M_P. The current quark mass m and the mass difference $M_N - M_P$ are both of MeV order and negligible when compared with the nucleon mass. The computation of the left-hand side is completed with the matrix element of γ_5 in the Dirac nucleon, which is g_A except for a possible phase. In what concerns the right-hand side of Eq. (30), the sum in the three internal quark lines produces the coupling of the pion to a nucleon. We do not need to be concerned with the interactions in the remaining diquark because they also dress the pion coupling to the nucleon. Excluding phases, Eq. (30) is then

$$2M_n g_A = \sqrt{2} g_{\pi nn} \frac{1}{P_1^2 - M_\pi^2} \sqrt{2} f_\pi (P_1^2 - M_\pi^2), \tag{31}$$

where P_1^μ is the momentum that flows in the pseudoscalar ladder, $-i\sqrt{2} g_{\pi nn}$ is the coupling of the pion to the nucleon (the $\sqrt{2}$ is a flavor factor), and the pion decay constant f_π is defined with the traces (13) and (28).

Equation (31) relates the nucleon decay with the pion decay constant, the famous Goldberger-Treiman relation [10],

$$M_n g_A = g_{n\pi n} f_\pi, \tag{32}$$

which is correct except for a small discrepancy of 6% [35,36]. This experimental verification suggests that the planar series of diagrams is acceptable, that the pseudoscalar ladder and the pion vertex can be used outside the mass shell, and that the expansion in P^μ and M_π is convergent.

VI. THE ADLER SELF-CONSISTENCY ZERO

Adler showed [11] that in the chiral limit of $m=0$, pions of vanishing momentum decouple from other mesons on the mass shell. In this limit [see Eq. (23)] the pion vertex is proportional to the dressed axial vertex, $\chi_\pi \alpha \Gamma_A$. Therefore I simply have to show that Γ_A decouples from loops with meson vertices. This decoupling is straightforward in a three-meson coupling,

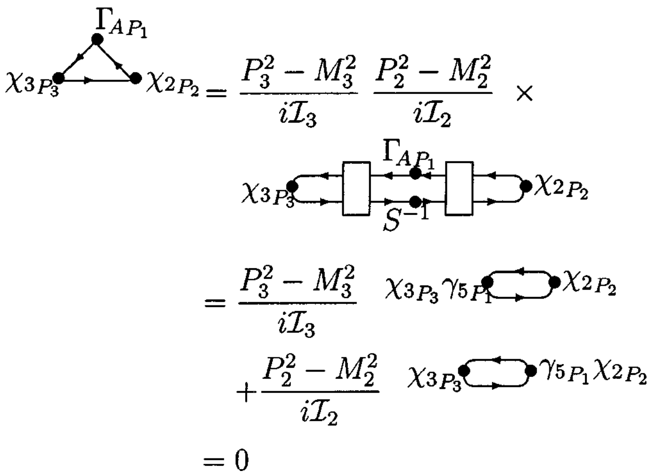

(33)

and this vanishes when the mesons of vertex χ_2 and χ_3 are on the mass shell. To get this result I used Eqs. (14) and (22). In the three meson coupling of Eq. (33) the Feynman loop is empty. Any planar insertion of the quark-quark interaction would produce double counting, because the vertices are already dressed.

However, the three-meson coupling is not the best one to find the direct evidence of an Adler zero. Because the mesons of vertex χ_2 and χ_3 couple to a pion, either the coupling is derivative or the mesons 1 and 2 have opposite parity. In the case of a derivative coupling the vanishing result is trivial, and it is not a PCAC result. In the case of opposite parity, and because chiral symmetry is spontaneously broken, the mesons 1 and 2 are not expected to have the same mass. Therefore, either 1 and 2 are not both on the mass shell, or the pion momentum in not vanishing, and Eq. (33) does not apply.

The four-meson coupling is more interesting than the three-meson one. If two pions are coupled to two identical mesons, then all four mesons can be on the mass shell. In the coupling of four mesons, the planar diagrams must be included, and they can be resummed in two different intermediate ladder exchanges,

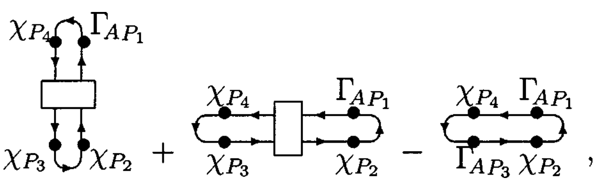

(34)

where the empty box is subtracted to cure double counting. I again follow the prescription defined in Sec. IV of excluding diagrams which would dress the quark-quark potential vertex V, the quark propagator $\mathcal{S}$, or the meson vertex χ_{P_i}. The intermediate ladders include both a direct contact term and the pole corresponding to meson exchange. There is also evidence that the hadron-hadron coupled-channel equations should include one meson exchange in the σ model [37], in the Nambu and Jona-Lasinio model [19], in the constituent quark models [4,5], and in a Euclidean quark model [4]. In microscopic calculations the Feynman loop of a four-meson coupling, which dominates for instance for π-π scattering, must therefore include inside the box a vertical scalar ladder and a horizontal scalar ladder [4].

The main step to get the zero consists in decreasing the number of vertices using again Eqs. (14) and (22). For instance I find that the second diagram of Eq. (34)

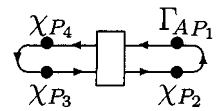

(35)

is identical to

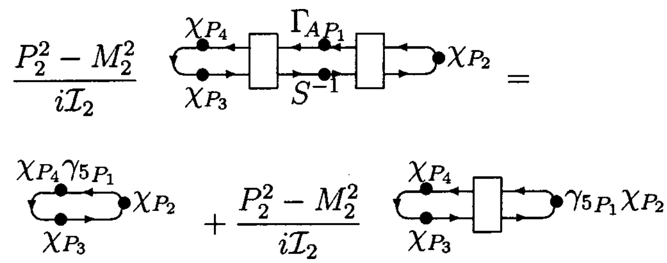

(36)

The first diagram of Eq. (34) is computed in the same way. The crucial step consists in realizing that in the sum of the three diagrams of Eq. (34), the empty loop, without intermediate ladders, exactly cancels due to Eq. (18). The sum of the three diagrams of Eq. (34) is exactly equal to

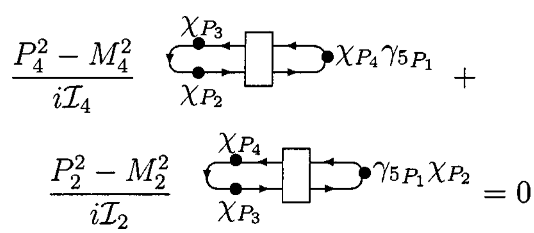

(37)

and this vanishes when the mesons of vertex χ_2 and χ_4 are on the mass shell. Although poles occur in the remaining intermediate ladder in Eq. (37), they are not expected to reside, say at $P_2^2=M_2^2$, because $\chi_2\gamma_{5P_1}$ has the opposite parity of χ_2, and because chiral symmetry is spontaneously broken.

The same method can be used to show that the pion *decouples from any number of mesons* on the mass shell. This constitutes a Ward identity for the meson couplings. The quark model complies with the Adler self-consistency zero.

VII. THE WEINBERG THEOREM

The four-pion coupling, which dominates π-π low-energy scattering, is the ideal process for which the Adler self-consistency zero applies. To find a nonvanishing contribution, the Feynman loop that extends Eq. (34) must be expanded up to first order in $P_i \cdot P_j$ and in M_π^2. The result is a beautiful algebraic expression that was first derived by Weinberg. After the original work of Weinberg [12], the theorem was also derived with Ward identities for the pion fields [38] and with a functional integration of quarks [39]. I now prove that the π-π scattering theorem of Weinberg [12] applies to quark models with chiral invariant quark-quark interactions, completing in full detail an analytical proof that was recently outlined in Refs. [4] and [5].

The most technical task of this paper consists in computing *independently of the quark model*, and up to order M_π^2 and P_iP_j in the π mass and momenta, the Feynman loop

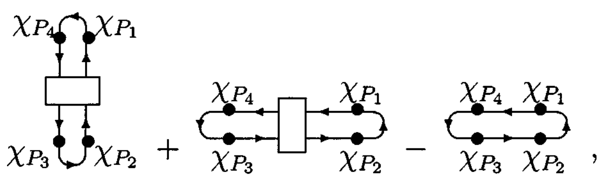

(38)

where χ is the Bethe-Salpeter vertex of the pion. The subindex P_i accounts for an external momentum flowing into the loop.

To get the loop (38) up to order $P_i \cdot P_j$ and M_π^2, at most two full Bethe-Salpeter vertices χ are needed. The other two can be approximated by $\Gamma_A/(2in_\pi)$, according to Eq. (25). Expanding the four χ, which are respectively equal to $\Gamma_A/(2in_\pi)+[\chi-\Gamma_A/(2in_\pi)]$, up to second order in $\chi-\Gamma_A/(2in_\pi)$ and regrouping the sum, one finds that the amplitude of Eq. (38) is the sum of four classes of terms. Each class includes a sum of the possible cyclic permutations of the external momenta P_1, P_2, P_3, and P_4. The sum of the four classes is identical to, with factor 3 times $(2in_\pi)^{-4}$,

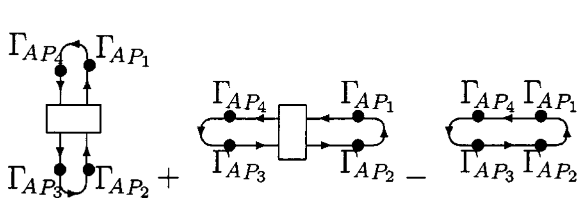

(39)

minus, with factor 2 times $(2in_\pi)^{-3}$ (four permutations),

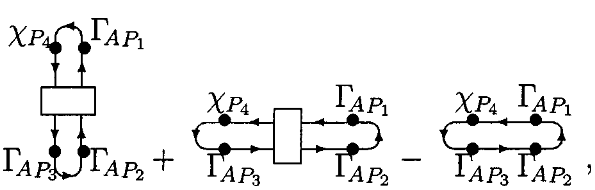

(40)

plus, with factor $(2in_\pi)^{-2}$ (four permutations),

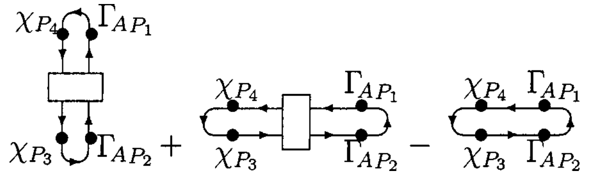

(41)

plus, with factor $(2in_\pi)^{-2}$ (two permutations),

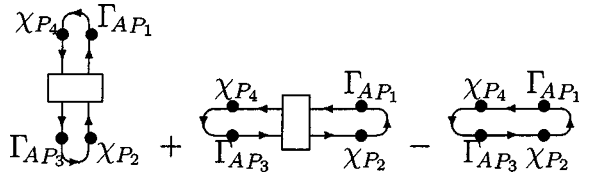

(42)

I now compute these diagrams up to the order of $P_i \cdot P_j$ and M_π^2, starting with the terms with move vertices χ_π, which are closer to the ones computed in Sec. VI.

A. The $\chi\Gamma_A\chi\Gamma_A$ amplitude

Here I compute the diagrams of Eq. (42). The first steps are identical to the ones of Sec. VI, and the diagrams are identical to the ones of Eq. (37) except that now the Bethe-Salpeter vertex χ_{P_3} is replaced by the axial vertex $\Gamma_{A_{P_3}}$,

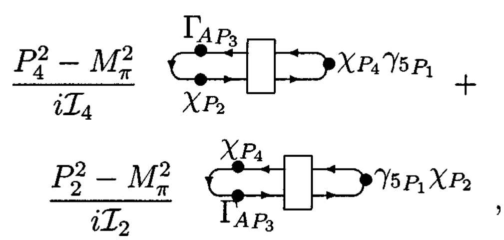

(43)

where it is convenient to use Eq. (14) to include the ladder in the adjacent χ_π,

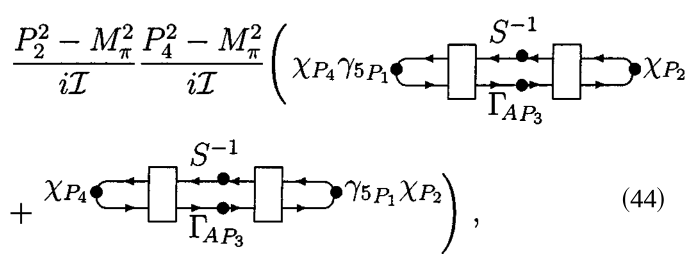

(44)

and to apply the Ward identity (22) to the axial vertex $\Gamma_{A_{P_3}}$,

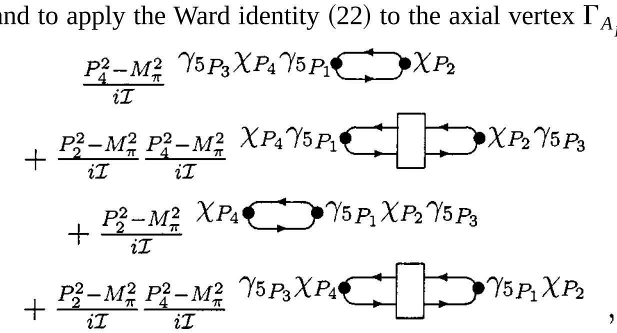

(45)

where this result is exact. Only the contribution up to order second order $P_i \cdot P_j$ or M_π^2 needs to be retained. In Eq. (45) there are two classes of diagrams. The second and fourth diagrams have scalar or vector vertices $\chi\gamma_5$, and therefore the ladder is not a pseudoscalar and is not able to cancel the higher-order factor $[(P_2^2 - M_\pi^2)/i\mathcal{I}][(P_4^2 - M_\pi^2)/i\mathcal{I}]$. The first and third diagrams, with a pseudoscalar vertex χ, already have a factor $(P^2 - M_\pi^2)/i\mathcal{I}$ of second order. Therefore the remaining trace $\mathrm{tr}\{\gamma_5\chi\gamma_5 S\chi S\}$ only needs to be computed at zero order where this trace is simply the constant $\mathcal{I}$ which was defined in Eq. (7). The final result up to second order is

$$\frac{P_2^2 - M_\pi^2 + P_4^2 - M_\pi^2}{i}. \tag{46}$$

B. The $\chi\chi\Gamma_A\Gamma_A$ amplitude

Here I compute the diagrams of Eq. (41). Again the first steps are similar to the ones of Sec. VI, and the diagrams are identical to the ones of Eq. (37) except that the Bethe-Salpeter vertex χ_{P_2} is replaced by the axial vertex $\Gamma_{A_{P_2}}$. In the second diagram of Eq. (41), the axial vertex $\Gamma_{A_{P_2}}$ is adjacent to the vertex $\Gamma_{A_{P_1}}$ and Eq. (21) substitutes for Eq. (14). The equation similar to Eq. (37) is now

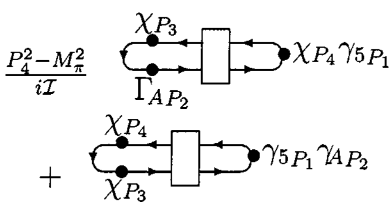

(47)

where the last term is already proportional to $\gamma_{A_{P_2}}$ so it only needs one of the χ to produce a term of second order. So in the last term it is convenient to return to a lower order in $\chi - (i/2f_\pi)\Gamma_A$, where $\chi\chi$ is replaced by $\chi(i/2f_\pi)\Gamma_A + (i/2f_\pi)\Gamma_A\chi - (i/2f_\pi)\Gamma_A(i/2f_\pi)\Gamma_A$. Including the desired ladders, there are four different terms:

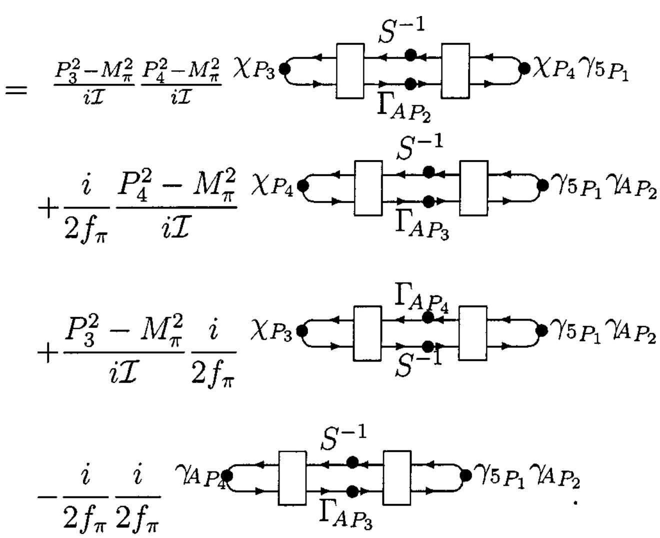

(48)

Using again the Ward identity (22), and removing the higher-order cases where the ladder is scalar, Eq. (47) simplifies to

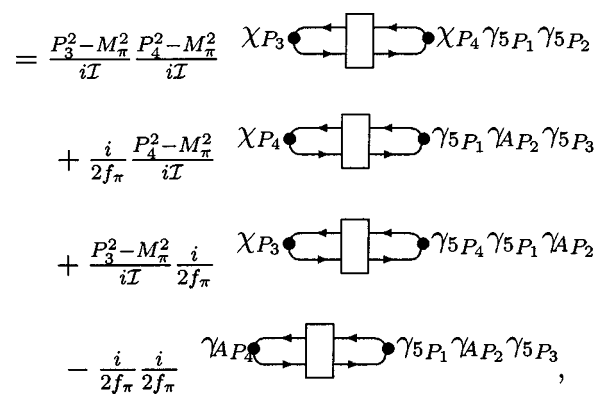

(49)

where the ladders can all be reabsorbed in vertices,

$$
\begin{aligned}
&= \frac{P_4^2 - M_\pi^2}{i\mathcal{I}}\mathrm{tr}\{(S\chi S)_{P_3}\chi_{P_4}\} + \frac{i}{2f_\pi}\mathrm{tr}\{(S\chi S)_{P_4}\gamma_{A-P_2}\}\\
&\quad + \frac{i}{2f_\pi}\mathrm{tr}\{(S\chi S)_{P_3}\gamma_{A_{P_2}}\} - \frac{i}{2f_\pi}\frac{i}{2f_\pi}\mathrm{tr}\{(S\Gamma_A S)_{P_4}\gamma_{A-P_2}\}\\
&= \frac{P_4^2 - M_\pi^2}{i} + \frac{P_4 \cdot P_2 - M_\pi^2}{i} + \frac{-P_3 \cdot P_2 - M_\pi^2}{i} - \frac{-M_\pi^2}{i}\\
&= \frac{P_3^2 + P_4^2 + P_3 \cdot P_4 + P_3 \cdot P_1 + P_4 \cdot P_2 - 2M_\pi^2}{i},
\end{aligned} \tag{50}
$$

and this is the final result of Eq. (41) up to second order.

C. The $\chi\Gamma_A\Gamma_A\Gamma_A$ amplitude

I now compute the diagrams of Eq. (40). The first step is identical to the previous case except that the Bethe-Salpeter vertex χ_{P_3} is replaced by the axial vertex $\Gamma_{A_{P_3}}$. The equation similar to Eq. (37) is now

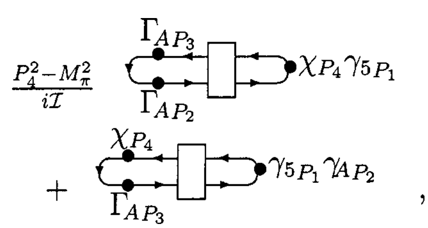

(51)

and the Ward identity (22) can now be used in the axial vertex $\Gamma_{A_{P_3}}$. Again Eqs. (14) or (21) are needed to introduce a second ladder in the loop. Excluding the terms with vertex scalar or vector vertex $\chi\gamma_5$ which have a higher order, Eq. (51) simplifies to

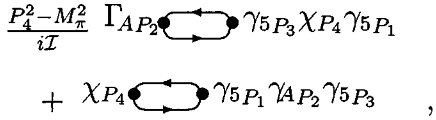
(52)

and this can be further simplified when only the second order is retained. Using Eq. (23) the zero order of the loop in the first diagram simplifies to $2in_\pi\mathcal{I}$. The second loop is computed with the trace (condensed). The result for Eq. (40) is

$$(2n_\pi)[(P_4+P_2)\cdot P_4-2M_\pi^2]. \tag{53}$$

D. Four Γ_A vertices

I now compute the diagrams of Eq. (39), where all the vertices are axial vertices $\Gamma_{A_{P_i}}$. The technique to simplify the loops is identical to the previous cases, but the term with a scalar or vector ladder must also be considered because it contributes to the second order. The number of vertices is again decreased with the help of Eqs. (22) and (21),

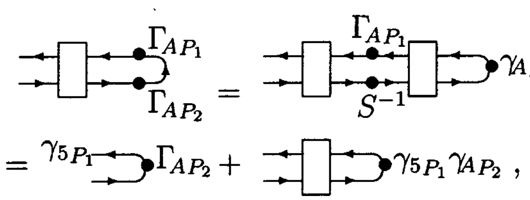
(54)

where the Ward identity (22) can also be applied to the vertex $\Gamma_{A_{P_2}}$, rather than be applied to the vertex $\Gamma_{A_{P_1}}$. It is more convenient to take the average of these two possible choices. This is repeated with the vertices $\Gamma_{A_{P_3}}$ and $\Gamma_{A_{P_4}}$ to compute the square box with ladder

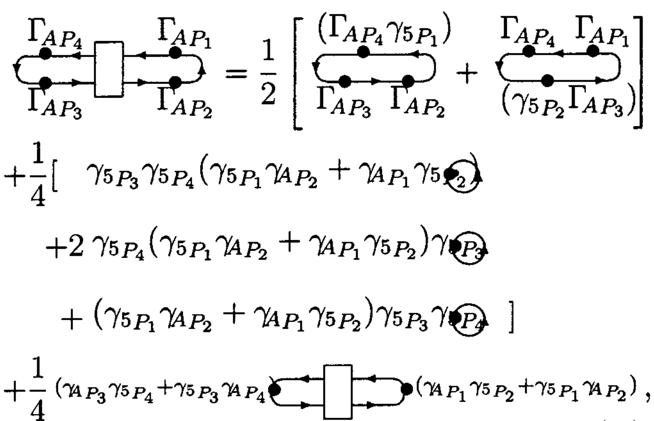
(55)

where there are three classes of terms, respectively, with zero, one, and two vertices γ_A. I note that all the other factors (Γ_A, S, and the scalar and vector ladder) are finite and carry the scale of the effective quark-quark interaction. The first term, with zero γ_A, cancels when the three diagrams of Eq. (39) are summed. Using Eq. (19), the second term of Eq. (55), with one γ_A, is

$$\frac{1}{4i}\mathrm{tr}\{(\not P_1-\not P_2)[S_{P_2,P_3}-2S_{P_3,P_4}+S_{P_4,P_1}] \\ -4m[S_{P_2,P_3}+2S_{P_3,P_4}+S_{P_4,P_1}]\}, \tag{56}$$

where the quark propagators S_{P_i,P_j} are indexed with the attached external momenta for book keeping. Expanding up to second order in P_i and M_π, and using the relation of Gell-Mann, Oakes, and Renner (29), Eq. (56) simplifies to

$$\frac{1}{4i}\mathrm{tr}\{(\not P_1-\not P_2)(P_3-P_4)^\mu\partial_\mu S\}-4if_\pi^2M_\pi^2. \tag{57}$$

The third term with of Eq. (55), with two γ_A vertices, is equal to

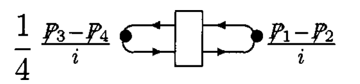
(58)

It is interesting to remark that the vector Ward identity cancels up to second order the momentum-dependent part of Eq. (57) with Eq. (58). The vector Ward produces equations comparable to Eqs. (18) and (21), in particular,

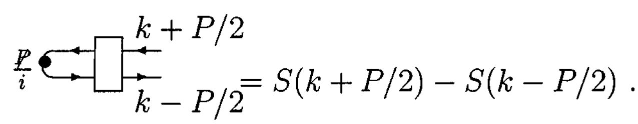
(59)

The expansion up to first order in P^μ of Eq. (59) produces

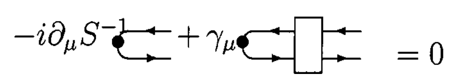
(60)

Therefore the sum of the momentum dependent parts of Eqs. (57) and (58)

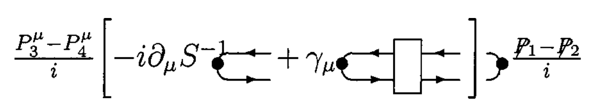
(61)

cancels due to the vector Ward identity (60). Only the constant term remains, and this is exact up to order P_iP_j. The final result for the Feynman diagrams of Eq. (39) is

$$-8in_\pi^2M_\pi^2. \tag{62}$$

E. Scattering parameters

Summing the contributions of Eqs. (46), (50), (53) and (62), the Feynman loop of Eq. (38) results in

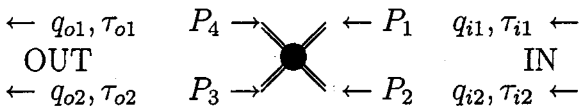

FIG. 3. To compute the T matrix for π-π scattering, the external momenta of the Feynman loop (38) must be matched with the incoming and outgoing pion momenta. There are six different possible combinations. The Feynman loop (38) is represented by the solid circle.

$$+3\left(\frac{1}{2in_\pi}\right)^4(-8in_\pi^2M_\pi^2)-2\left(\frac{1}{2in_\pi}\right)^3\sum_{4\ \text{perm}}2n_\pi(P_1^2+P_1\cdot P_3-2M_\pi^2)+\left(\frac{1}{2in_\pi}\right)^2\sum_{4\ \text{perm}}\times\frac{P_1^2+P_2^2+P_1\cdot P_2+P_1\cdot P_3+P_2\cdot P_4-2M_\pi^2}{i}+\left(\frac{1}{2in_\pi}\right)^2\sum_{2\ \text{perm}}\frac{P_1^2+P_3^2-2M_\pi^2}{i}$$

$$=\frac{i}{2f_\pi^2}[(P_1+P_2)^2+(P_1+P_4)^2-2M_\pi^2], \tag{63}$$

where the conservation $P_1+P_2+P_3+P_4=0$ of momentum was used to simplify the result.

I finally compute the π-π scattering matrix T. The external pions, $i1$ and $i2$ incoming and $o1$ and $o2$ outgoing, are simply matched with the four pion vertex that I just computed in Eq. (63). This is depicted in Fig. 3, where the loop (38) is represented by the solid circle. The loop is topologically invariant for cyclic permutations of P_1, P_2, P_3, and P_4. To remove double counting one match is fixed, say $P_1=q_{i1}$. Then there are six different combinations of the remaining external legs,

neighbor:

$$P_1=q_{i1},\quad P_2=q_{i2},\quad P_3=-q_{o2},\quad P_4=-q_{o1};$$
$$P_1=q_{i1},\quad P_2=q_{i2},\quad P_3=-q_{o1},\quad P_4=-q_{o2};$$
$$P_1=q_{i1},\quad P_2=-q_{o1},\quad P_3=-q_{o2},\quad P_4=q_{i2};$$
$$P_1=q_{i1},\quad P_2=-q_{o1},\quad P_3=q_{i2},\quad P_4=-q_{o2};$$

separated:

$$P_1=q_{i1},\quad P_2=-q_{o2},\quad P_3=q_{i2},\quad P_4=-q_{o1};$$
$$P_1=q_{i1},\quad P_2=-q_{o2},\quad P_3=-q_{o1},\quad P_4=q_{i2}; \tag{64}$$

where in the first four combinations the incoming pions are *neighbors* in the Feynman loop, while in the last two combinations the incoming pions are *separated* in the quark loop by an outgoing pion.

In what concerns color, all the combinations are identical because the pion is a color singlet, and the color factor is appropriately included in the definition of f_π [see Eq. (13)]. With regard to momentum, the result is expressed in the usual Mandelstam relativistic invariant variables s, t, and u. For instance, the first combination in Eq. (64) produces the result $i(s+u-2M_\pi^2)/(4f_\pi^2)$. I now introduce flavor. For compactness it was not regarded in the previous definitions of the vertices Γ_{A_P} and χ_P. Because the pion is an isovector, there are three different cases: $I=0$, $I=1$, and $I=2$. The flavor contributions to the pion vertex simply factorize from the momentum contribution, and the different combinations only produce two classes of flavor traces, which correspond to the *neighbor* and *separated* classes in Eq. (64). The flavor results are compiled in Table I. Summing the six possible combinations of color, spin, momentum, and flavor traces, and dividing by $-i$, the π-π scattering T^I matrices are finally

TABLE I. Table of the flavor traces. $\mathrm{tr}\{\tau_{i1}\tau_{i2}\tau_{o2}^\dagger\tau_{o1}^\dagger\}$ and $\mathrm{tr}\{\tau_{i1}\tau_{o2}^\dagger\tau_{i2}\tau_{o1}^\dagger\}$ are examples of the neighbor and separated cases.

Im_I	$\tau_{i1}\tau_{i2}$	Neighbor	Separated
00	$\frac{\vec{\sigma}\cdot\vec{\sigma}}{2\sqrt{6}}$	$\frac{3}{4}$	$-\frac{1}{4}$
11	$\frac{\sigma_1\sigma_2-\sigma_2\sigma_1}{4}$	$\frac{1}{2}$	0
22	$\frac{\sigma^+\sigma^+}{\sqrt{2}}$	0	$\frac{1}{2}$

$$T^0=-\frac{2s-M_\pi^2}{2f_\pi^2}-\frac{s+t+u-4M_\pi^2}{2f_\pi^2},$$
$$T^1=-\frac{t-u}{2f_\pi^2}, \tag{65}$$
$$T^2=-\frac{-s+2M_\pi^2}{2f_\pi^2}-\frac{s+t+u-4M_\pi^2}{2f_\pi^2},$$

where $s+t+u-4M_\pi^2$ expresses the off-mass-shell contribution. The T^I matrices of Eq. (65) are computed at the tree level (including scalar and vector s, t, and u exchange), which is exact up to the order of $P_i^2P_j^2$ and of M_π^2. Equation (65) complies with the Gasser and Leutwyler results [38]. Off-mass-shell effects are very important for the experiments. For instance, in the scattering at π-π threshold of a π beam with virtual π^* provided by a nucleon target [40], the off-mass-shell effects of Eq. (65) decrease T^0 by a factor of 0.5 and increase T^2 by a factor of 1.7.

The π-π scattering lengths a_0^I are simply obtained from the mass-shell scattering amplitudes T^0 and T^2 with the Born factor of $-1/16\pi M_\pi$, and for vanishing three-momenta. The $I=1$ case is antisymmetric so the first scattering parameter is a_1^1 and the corresponding factor is $(-1/16\pi M_\pi)\times[4/3(t-u)]$,

$$a_0^0 = \frac{7}{32\pi}\frac{M_\pi}{f_\pi^2},$$

$$a_1^1 = \frac{1}{24\pi}\frac{1}{M_\pi f_\pi^2}, \tag{66}$$

$$a_0^2 = \frac{-1}{16\pi}\frac{M_\pi}{f_\pi^2};$$

this is the result of the famous Weinberg theorem for π-π scattering [12].

For simplicity, renormalization [28,41] was omitted from the details of this paper, and all the Feynman loops were assumed to be finite. Nevertheless the results are not affected by the use of an ultraviolet divergent kernel, say by the one-gluon exchange interaction $K(q)\alpha 1/q^2$ which renders the integral in Eq. (15) logarithmicly divergent. The same renormalization of ultraviolet divergences also occurs in atomic physics, where the spectrum and the cross section of atoms are simply not affected by the divergences which are present in the Shwinger-Dyson equation of QED. Following Ref. [28], the divergent integral is regularized with an ultraviolet cutoff Λ_{uv}, and the dressed propagator is renormalized in Eq. (15) by the quark wave function renormalization factor of Z_2 and by the vertex renormalization factor of Z_1. The axial Ward identity (18), the vector Ward identity (60), and the normalization condition of the Bethe-Salpeter vertex (11) ensure that the axial vertex Γ_A, the vector vertex V, and the normalization condition of the Bethe-Salpeter vertex χ_π get the same renormalization factor, which coincides with the inverse of the renormalization factor of the quark propagator. Thus the Adler zero and the Weinberg result, which are computed in Feynman loops with an identical number of quark propagators and vertices (axial, vector or Bethe-Salpeter), are insensitive to the renormalization factors. The results maintain the same expressions in terms of the physically observable M_π and f_π, which are not affected by the ultraviolet infinities in the renormalization factors.

VIII. CONCLUSION

In this paper a low momentum and chiral expansion is performed on amplitudes computed in the framework of the quark model with chiral symmetry breaking. The expansion is analytical, and dressed Feynman diagrams are used for the compactness of the expansion. The axial Ward identities, including a nontrivial Ward identity for the ladder, and the vector Ward identity are essential tools to arrive at simple and model independent results.

A detailed proof is shown, which confirms that Goldstone bosons not only are massless, in agreement with the relation of Gell-Mann, Oakes, and Renner, but also that Goldstone bosons are noninteracting at low energy in agreement with the Adler self-consistency zeros. This proof also confirms that intermediate ladders, which describe both meson exchanges and contact terms, must be included in low energy quark loops.

Moreover, this paper verifies that the famous PCAC relations of Goldberger and Treiman and of Weinberg are also obtained when the pions are off the mass shell and have a finite size. The quark model provides a well-defined prescription for the exchange of virtual intermediate off-mass-shell pions.

The most involved technical part of this paper consists in detailing and completing the proof of the Weinberg theorem [12], which was recently published [4,5,42], and in extending the proof to off-mass-shell pions. Other important precursors of this work are the study of π-π scattering [19] in the Nambu and Jona-Lasinio model, and the study of π-π scattering with the bosonization method [39].

It is a remarkable achievement of chiral symmetry that the quark propagator, the geometrical series of the ladder and the pion Bethe-Salpeter vertex, which are functions of the finite scale of the interaction, say the string tension σ or Λ_{QCD}, of the current quark mass m and of the ultraviolet cutoff Λ_{uv} explicitly disappear from the final results, which are simple functions of f_π and M_π only. Any quark model with a chirally symmetric interaction complies with the PCAC relations. This result is general and model independent.

I expect that the analytical techniques used here may also be applied to address other chiral effects within the quark model framework. The determination of the next-order terms in the pion momenta expansion of the π-π scattering amplitude will compute the l_1 and l_2 parameters of chiral Lagrangians, and will also tests quark models [43]. Another different extension of this paper would consist in addressing the anomalous axial Ward identities. The bosonization method suggests [44] that the Wess-Zumino term of the pion effective Lagrangean [45,46], which includes the Levi-Civita symbol $\epsilon^{\mu\nu\alpha\beta}$, say in the coupling of five pions [44], and the anomalous coupling of pions to photons [47–49] can also be studied within this framework.

ACKNOWLEDGMENTS

I mainly acknowledge Emilio Ribeiro for reporting on nontrivial Ward identities, and I am grateful to Felipe Llanes for correcting details in this manuscript. I also acknowledge discussions with Steve Cotanch, Gastão Krein, Felipe Llanes, Brigitte Hiller, Pieter Maris, Gonçalo Marques, Emilio Ribeiro, and Adam Szczepaniak.

[1] A. De Rujula, H. Georgi, and S. L. Glashow, Phys. Rev. D **12**, 147 (1975).
[2] J. Ribeiro, Z. Phys. C **5**, 27 (1980).
[3] P. Bicudo, G. Krein, and J. Ribeiro, Phys. Rev. C **64**, 025202 (2001).
[4] P. Bicudo, S. Cotanch, F. Llanes-Estrada, P. Maris, E. Ribeiro, and A. Szczepaniak, Phys. Rev. D **65**, 076008 (2002).
[5] P. Bicudo, M. Faria, G. Marques, and J. Ribeiro, nucl-th/0106071.
[6] A. Le Yaouanc, L. Oliver, O. Pene, and J.-C. Raynal, Phys.

Rev. D **29**, 1233 (1984); A. Le Yaouanc, L. Oliver, S. Ono, O. Pene, and J.-C. Raynal, *ibid.* **31**, 137 (1985).
[7] S. Adler and A. Davis, Nucl. Phys. **B244**, 469 (1984).
[8] P. Bicudo and J. Ribeiro, Phys. Rev. D **42**, 1611 (1990); **42**, 1625 (1990); **42**, 1635 (1990).
[9] M. Gell-Mann, R. J. Oakes, and B. Renner, Phys. Rev. **175**, 2195 (1968).
[10] M. L. Goldberger and S. B. Treiman, Phys. Rev. **111**, 354 (1958).
[11] S. L. Adler, Phys. Rev. **137**, B1022 (1965).
[12] S. Weinberg, Phys. Rev. Lett. **17**, 616 (1966).
[13] S. R. Amendolia *et al.*, Phys. Lett. B **146**, 116 (1984); E. B. Dally *et al.*, Phys. Rev. Lett. **48**, 375 (1982).
[14] G. Colangelo, in talk presented at the Confinement and Hadron Spectrum V, Gargnano, Italy, 2002, edited by N. Brambilla and G. Prosperi (World Scientific, Singapore, 2003).
[15] V. Yazov, in talk presented at the Confinement and Hadron Spectrum V, Gargnano, Italy, 2002, edited by N. Brambilla and G. Prosperi (World Scientific, Singapore, 2003).
[16] P. Estabrooks and A. D. Martin, Nucl. Phys. **B79**, 301 (1974).
[17] C. Llewellyn-Smith, Nuovo Cimento A **60**, 348 (1969).
[18] Y. Nambu and J. Jona-Lasinio, Phys. Rev. **124**, 246 (1961); **122**, 345 (1961).
[19] V. Bernard, U. G. Meissner, A. Blin, and B. Hiller, Phys. Lett. B **253**, 443 (1991); V. Bernard, A. H. Blin, B. Hiller, Y. P. Ivanov, A. A. Osipov, and U. Meissner, Ann. Phys. (N.Y.) **249**, 499 (1996).
[20] Y. Dai, C. Huang, and D. Liu, Phys. Rev. D **43**, 1717 (1991).
[21] C. D. Roberts and S. M. Schmidt, Prog. Part. Nucl. Phys. **45**, S1 (2000).
[22] R. Alkofer and L. von Smekal, Phys. Rep. **353**, 281 (2001).
[23] V. Sauli, hep-ph/0108160.
[24] J. Villate, D.-S. Liu, J. Ribeiro, and P. Bicudo, Phys. Rev. D **47**, 1145 (1993).
[25] W. Marciano and H. Pagels, Phys. Rep. **36**, 137 (1978).
[26] R. Delbourgo and M. D. Scadron, J. Phys. G **5**, 1621 (1979).
[27] P. Bicudo, Phys. Rev. C **60**, 035209 (1999).
[28] P. Maris, C. Roberts, and P. Tandy, Phys. Lett. B **420**, 267 (1998).
[29] M. A. Ivanov, Yu. L. Kalinovsky, and C. D. Roberts, Phys. Rev. D **60**, 034018 (1999).
[30] P. Maris, in *Quark Confinement and the Hadron Spectrum IV*, edited by W. Lucha and K. Maung Maung (World Scientific, Singapore, 2002).
[31] M. B. Hecht, C. D. Roberts, and S. M. Schmidt, in *Quark Confinement and the Hadron Spectrum IV*, edited by W. Lucha and K. Maung Maung (World Scientific, Singapore, 2002); P. Maris, A. Raya, C. D. Roberts, and S. M. Schmidt, nucl-th/0208071.
[32] J. C. R. Bloch, C. D. Roberts, and S. M. Schmidt, Phys. Rev. C **61**, 065207 (2000).
[33] P. Maris and P. C. Tandy, Phys. Rev. C **61**, 045202 (2000); **62**, 055204 (2000); **65**, 045211 (2002).
[34] C.-R. Ji and P. Maris, Phys. Rev. D **64**, 014032 (2001).
[35] H. Pagels, Phys. Rev. **179**, 1337 (1969).
[36] N. Ishii, Nucl. Phys. **A689**, 793 (2001).
[37] V. De Alfaro, S. Fubini, G. Furlan, and C. Rosseti, *Currents in Hadron Physics* (North-Holland, Amsterdam, 1973).
[38] J. Gasser and H. Leutwyler, Ann. Phys. (N.Y.) **158**, 142 (1984).
[39] C. Roberts, R. Cahill, M. Sevior, and N. Iannella, Phys. Rev. D **49**, 125 (1994).
[40] L. J. Gutay, F. T. Meiere, and J. H. Scharenguivel, Phys. Rev. Lett. **23**, 431 (1969).
[41] A. Szczepaniak and E. Swanson, Phys. Rev. D **55**, 1578 (1997); **62**, 094027 (2000); Phys. Rev. Lett. **87**, 072001 (2001).
[42] S. Cotanch and P. Maris, hep-ph/0210151.
[43] F. Llanes-Estrada and P. Bicudo, in *Quark Confinement and the Hadron Spectrum V*, edited by N. Brambilla and G. Prosperi (World Scientific, Singapore, 2002).
[44] J. Praschifka, C. D. Roberts, and R. T. Cahill, Phys. Rev. D **36**, 209 (1987); C. D. Roberts, R. T. Cahill, and J. Praschifka, Ann. Phys. (N.Y.) **188**, 20 (1988).
[45] J. Wess and B. Zumino, Phys. Lett. **37B**, 95 (1971).
[46] E. Witten, Nucl. Phys. **B223**, 422 (1983).
[47] Ö. Kaymakcalan, S. Rajeev, and J. Schechter, Phys. Rev. D **30**, 594 (1984); H. Gomm, Ö. Kaymakcalan, and J. Schechter, Phys. Rev. D **30**, 2345 (1984); Ö. Kaymakcalan and J. Schechter, Phys. Rev. D **31**, 1109 (1985).
[48] M. Bando, M. Harada, and T. Kugo, Prog. Theor. Phys. **91**, 927 (1994).
[49] C. D. Roberts, Nucl. Phys. **A605**, 475 (1996); R. Alkofer and C. D. Roberts, Phys. Lett. B **369**, 101 (1996); P. Maris and C. D. Roberts, Phys. Rev. C **58**, 3659 (1998).